Different continuum approaches to giant resonances in ^{208}Pb with 400-MeV protons

L. W. Swenson and X. Y. Chen
Oregon State University, Corvallis, Oregon 97330

J. Lisantti,* D. K. McDaniels, and I. Bergqvist
University of Oregon, Eugene, Oregon 97403

F. E. Bertrand, D. J. Horen, E. E. Gross, C. Glover, R. O. Sayer, and B. L. Burks
Oak Ridge National Laboratory, Oak Ridge, Tennessee 37831

O. Häusser,† K. Hicks, and M. J. Iqbal
Tri-Universities Meson Physics Facility, Vancouver, British Columbia, Canada V6T 2A3
(Received 28 December 1987)

New ^{208}Pb(p,p') measurements at 400 MeV are reported and analyzed using new approaches to the continuum in the giant resonance region. These approaches include a phenomenological procedure, and calculations based on the free surface response function of semi-infinite nuclear matter. These methods are found to lead to giant resonance parameters which are consistent and in agreement with established results. We interpret this to mean that both approaches provide empirically consistent representations of the continuum underlying the giant resonances. In addition to the well-known resonances, evidence of possible $3\hbar\omega$ $L=5$ resonance strength is observed at 18-MeV excitation accounting for 10 ± 3 % of the energy-weighted sum rule.

I. INTRODUCTION

During the past few years several studies[1–9] have demonstrated the usefulness of inelastic proton scattering at medium energies for the study of giant resonances. Features that make these investigations so successful include clean spectra with large peak-to-continuum ratios and selectivity to angular momentum transfer. Good peak-to-continuum ratios and a reliable method of determining the underlying continuum or background are necessary to properly extract giant resonance parameters such as excitation energy, width, and energy-weighted sum rule (EWSR) fractions. Additionally, medium-energy inelastic-proton scattering has the advantage that angular distributions for various L transfers peak at considerably different angles. This latter feature allows more certain identification of resonance multipolarity than for many other probes.[10] Collective model distorted-wave Born approximation (DWBA) calculations on which these angular distributions are based have recently been shown to correctly describe the excitation of both the known giant resonances[7,9] in ^{208}Pb, and the well-known low-lying collective states.[11]

While the parameters of the lower-lying isoscalar giant quadrupole (ISGQR), giant monopole (ISGMR), and isovector giant dipole (IVGDR) resonances have been established with a variety of hadronic and electromagnetic probes, the exact multipolarity composition of resonances in the excitation region above the IVGDR (14 MeV) in ^{208}Pb is still uncertain. Measurements[12,13] made with 172-MeV alpha particles were interpreted as showing evidence of an isoscalar giant octupole (ISGOR) resonance at 17.5–18.7 MeV and measurements made with 340- and 480-MeV alpha particles find $L=3$ strength in the 18–23-MeV region.[14] The $3\hbar\omega$ ISGOR is, however, often partially obscured in low-energy (α,α') experiments because of breakup following neutron and proton pickup reactions. Support for a ISGOR at 17.5 MeV is also given by a (p,p') experiment[4] performed with 201-MeV protons. Our own recent (p,p') experiment[7] at 200 MeV shows a preference for locating the ISGOR at 20.9 MeV. An experiment[2] with 800-MeV protons reported that the ISGOR is located near 19.1 MeV, while a 120-MeV (^{3}He,^{3}He′) measurement[15] favored an excitation energy of 20.5 MeV. Evidence for $L=5$, $3\hbar\omega$ strength in a broad region around 21 MeV excitation has also been reported[14] in (α,α') experiments at 340 and 480 MeV. In this same region evidence for isoscalar giant dipole (ISGDR) strength, a compressional mode of excitation, has been reported at 21.3 MeV in 172 MeV alpha-particle experiments.[12] In addition, the isovector quadrupole (IVGQR) is expected in the same region[16] of excitation. The ISGDR and IVGQR cannot be distinguished in (p,p') measurements at forward angles. The combination has been observed at 21.5 MeV with 201-MeV protons[4] and at 22.6-MeV excitation with 800-MeV protons.[8]

The broader resonances in this region, 16–24 MeV in ^{208}Pb, are more difficult to recognize, and extraction of their EWSR strength depends upon the assumed or calculated underlying background. Current progress in determining the parameters of these interesting giant resonances is closely coupled with progress in modeling the nuclear continuum. The empirical procedure often used in the past consists of representing the continuum shape

with straight lines or smooth polynomial curves incorporating a criterion of "reasonableness." Different choices of background can, however, lead to quite different resonance parameters, especially the EWSR fraction. Clearly there is a need for a consistent description of the continuum based on some assumption about the underlying reaction mechanism.

As a starting point in formulating a model for the continuum, quasielastic scattering may be assumed to be the dominant contributing process. The observed kinematics and analyzing power of the continuum support this view. From (p,p') measurements[17] at 200 MeV on ^{60}Ni, ^{90}Zr, and ^{208}Pb the broad structure underlying the giant resonances is observed to move in excitation energy in accordance with nucleon-nucleon (NN) scattering kinematics, modified to include a small energy shift. For scattering angles less than 20°, the analyzing power for the continuum at the quasifree peak location was observed to be somewhat less than the free NN values at 200 MeV (Ref. 17), a little larger at 334 MeV (Ref. 18), and nearly the full NN value at 800 MeV.[19] Thus, observations of both kinematics and analyzing power support the view that the continuum is dominated by quasifree scattering, at least for moderate excitation energies and momentum transfer.

The above interpretation of a single step process in the continuum led us to develop an improved phenomenological procedure. In this procedure the continuum in the giant resonance region at excitation energies at and below the quasielastic peak was described by a Gaussian function, connected smoothly to a fourth-order polynomial for excitation energies above the quasielastic peak. This procedure was used successfully in analyzing our 200-MeV data[7] leading to a value for the ISGQR EWSR strength in agreement with previous measurements.

Recently, significant progress has been made in analytically describing the nuclear continuum. Esbensen and Bertsch[20] have formulated a model for the surface response of semi-infinite nuclear matter to represent the smoothed behavior of inclusive (p,p') scattering. Their calculation is based on a single-step scattering process that utilizes free NN scattering amplitudes. A detailed comparison with (p,p') data was made recently by the same authors[21] using both the total response and free response predictions calculated in slab geometry.[22] A relativistic model of the continuum has been developed by Horowitz and Iqbal[23] based on quasielastic scattering and takes account of medium effects through the use of the Dirac equation.

The focus of this paper is to compare the predictions of these continuum descriptions with inclusive spectra measured with 400-MeV protons scattered from ^{208}Pb. The resulting giant resonance parameters obtained will be compared along with results from other experiments. Our objective is to see if these continuum models give an accurate and consistent description of the background continuum in the giant resonance region, and if the extracted giant resonances are also appropriately accounted for in terms of their known excitation energies, widths, and EWSR fractions. Additionally, with these continuum models we seek a more reliable multipole decomposition and EWSR fraction determination for less well established resonances in the 16–24 MeV region for ^{208}Pb.

The experimental details of the present measurements are described in the next section. In Sec. III the surface response model is outlined. This section also contains a brief description of the relativistic impulse approximation approach and a phenomenological procedure for describing the continuum. The important results are summarized in Sec. IV, while the last section contains our discussion and conclusions.

II. EXPERIMENTAL

All measurements were performed at TRIUMF (Tri-Universities Meson Physics Facility). Protons of 400 MeV were extracted from the cyclotron with a beam current varying between 0.1–2.0 nA. Particles scattered from ^{208}Pb were detected with the upgraded Medium Resolution Spectrometer (MRS). The MRS has been described elsewhere[7] and only a few important features will be mentioned here.

At the entrance to the spectrometer the scattered particles pass through a low pressure wire chamber. One important function of this front-end chamber is to define the solid angle acceptance of the spectrometer which is of great value in making reliable cross section determinations. Along with the focal-plane vertical drift chambers the front-end chamber provides the capability of complete ray tracing back to the target, and consequently background free event selection. As a result "clean" spectra free of instrumental background were obtained. The resolution obtained for this experiment was 230 KeV (full width at half maximum, FWHF) for a 50 mg/cm^2 Pb target.

Another important feature of the MRS is its large momentum acceptance of $\pm 10\%$. The large acceptance feature is particularly important for studying higher multipole resonances. For 400-MeV protons, excitation energies of up to 80 MeV can be studied with one magnet setting. During this experiment emphasis was placed on inelastic scattering to low-lying states and to the giant resonance region up to 40 MeV. No analysis was done on the data above 40 MeV of excitation because of poor statistics.

In all (p,p') experiments elastic scattering measurements play an important role. Elastic data are required in order to obtain the necessary optical-model parameters for collective model DWBA calculations. It has been shown that the transition strengths obtained with the collective model are rather sensitive to the optical-model parameters used in the DWBA calculations.[9] Fortunately, at 400 MeV an extensive set of ^{208}Pb elastic scattering cross section and analyzing power data already exists.[24] This elastic data along with 200 and 300 MeV data were used in a global search for optical-model parameters.[9] In the present work we have used the 400-MeV average geometry potentials of Ref. 9. In order to obtain reliable cross-section normalizations and as a check of the scattering angle calibration, the elastic scattering cross sections measured in the present experiment were compared to those of D. A. Hutcheon *et al.*[24] This has proven to be the most reliable check of our absolute cross-

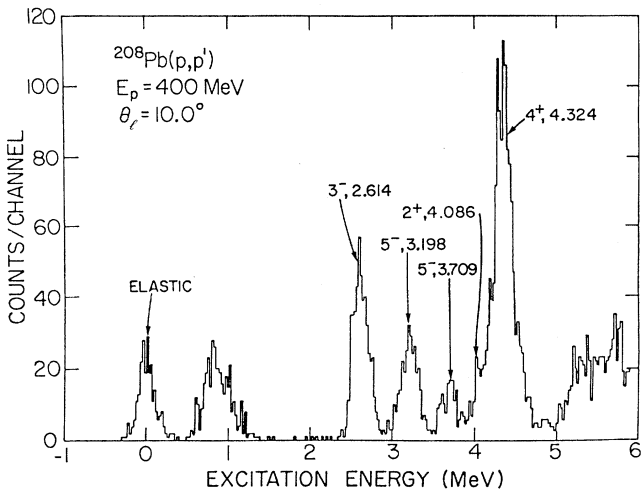

FIG. 1. Spectrum of 400-MeV protons scattered from a ^{208}Pb target at the laboratory angle 10°. The contaminant peak near 1 MeV of excitation was due to scattering from the target frame. The elastic peak has been prescaled by a factor of 256.

section determinations.

To accumulate inelastic scattering data efficiently it is necessary to suppress the elastic scattering, especially at forward angles. This was accomplished by placing an elastic veto scintillation counter at the appropriate position in the focal plane so that it intercepted only elastic events. As a result an extraneous peak in the 0–2-MeV range of excitation energy often appears in the spectra, which corresponds to events in the low-energy tail of the elastic peak, which sometimes miss the edge of the elastic veto counter. Beam scattered from the target frame contributes to the low-energy tail. This contribution presented no difficulty for the analysis of the data. Good, clean inelastic scattering peaks for the resolved low-lying collective states $3^-(2.614)$, $5^-(3.198)$, and $5^-(3.709)$ were always obtained as exhibited in Fig. 1. In order to check the spectra for target related problems, runs were occasionally made with only a blank frame in place. The contaminant was only observed in the 0–2-MeV range.

III. CONTINUUM MODELS

As noted in the Introduction, the continuum background under giant resonances appears to be dominated by quasifree scattering. In this study we take the approach of analyzing the data using three different models for the continuum, each based on the dominance of quasifree scattering. The first to be described will be the surface response model. The second is a relativistic model and the third a phenomenological approach to the continuum.

Recently significant progress has been made in the theoretical description of the nuclear continuum in model calculations by Bertsch, Scholten, Esbensen, and Smith.[20–22,25,26] The calculations are based on the surface response of semi-infinite nuclear matter, the free NN elastic scattering amplitude, and Glauber theory. In the surface response model[20–22] the double differential cross section for inelastic proton-nucleus scattering is given in factorized form by the relation

$$\frac{d^2\sigma}{d\Omega\, dE} = N_{\rm eff} \sum_{T,S} \left[\frac{d\sigma_{\rm NN}}{d\Omega} \right]_{T,S} S(q,E) \ . \tag{1}$$

A detailed description of the three factors contained in Eq. (1) is given Refs. 20–22. We mention here only some of the more important features.

The effective number of target nucleons $N_{\rm eff}$ is determined by Glauber theory for single scattering,

$$N_{\rm eff} = \int d^2\mathbf{b}\, n(b) e^{-n(b)\sigma_{\rm NN}} \ , \tag{2}$$

where $\sigma_{\rm NN}$ is the total NN cross section and

$$n(b) = \int_{-\infty}^{\infty} dx\, \rho_A (x^2+b^2)^{1/2} \ , \tag{3}$$

i.e., the number of target nucleons per fm^2 along a straight-line trajectory at an impact parameter b with respect to the center of the target nucleus of density ρ_A. The term in the exponential of Eq. (2) serves as a damping factor and is related to the mean-free path of a nucleon in the nucleus. Distortions in the scattering are simulated in this manner. As pointed out in Ref. 21 the factor $n(b)$ assumes a straight line trajectory through the nucleus and hence may not be appropriate for large scattering angles. In the present application at 400 MeV we take $\sigma_{\rm NN}=27$ mb, which gives $N_{\rm eff}=15$ for all angles. This factor is to be regarded as an overall scaling factor in the model.

In Eq. (1) $d\sigma_{\rm NN}/d\Omega$ represents the free differential nucleon-nucleon cross section. The representation of Wallace[27] was utilized, which pertains to free NN scattering as was the case in Ref. 20.

The surface response function $S(q,E)$, which is a function of the momentum transfer q and the excitation energy E_x, is obtained from the Green's function for particle-hole excitations in semi-infinite nuclear matter. The surface response is generated by an external field chosen to be consistent with Glauber theory. Details of the response function calculation can be found in Ref. 20. The external field contains a plane wave associated with the z component (perpendicular to the surface of the semi-infinite slab in the model of Ref. 22) of the momentum transfer q to the incoming proton. It has the form

$$V(z) = F(z) e^{iq_z Z} \ . \tag{4}$$

The function $F(z)$ contains the effect of absorption in the nuclear interior.

The response function has been shown[21] to be relatively insensitive to the target or beam energy via the field $F(z)$. The target dependence is mainly contained in the factor $N_{\rm eff}$, whereas the energy dependence is contained in the differential NN cross section and in $N_{\rm eff}$ though the total NN cross section.

The value of the total cross section $\sigma_{\rm NN}$ that enters into the Glauber calculation has usually been taken from the free scattering. However, $\sigma_{\rm NN}$ should be modified to account for medium effects such as Pauli blocking and re-

sidual particle-hole interactions. The free surface response corresponds to neglecting the residual interactions, and has been shown to be a reasonable approximation for the study of the nuclear continuum with 300–800-MeV protons.[21]

A relativistic version of the continuum calculations has been developed by Horowitz and Iqbal[23] based on the Dirac equation. In those calculations $\sigma_{NN}(\theta)$ is modified to include the enhancement of the lower components of the Dirac wave function in the nuclear medium which may be characterized by the introduction of an effective mass M^* which depends on the nuclear density. For ^{208}Pb, those authors calculated M^* to be about $0.83M$. The nuclear response was calculated using a Fermi gas approximation.

A phenomenological approach to the continuum has been developed from our previous experience analyzing the 200-MeV data[7] on ^{208}Pb. In this analysis the low-energy portion of the continuum was described by a Gaussian whose centroid excitation energy is given by

$$E_x = T_0 - \left[\frac{(T_0+V_0-B)\cos^2\theta}{1+\frac{T_0+V_0}{2mc^2}\sin^2\theta} - V_0 \right] . \quad (5)$$

The term in brackets corresponds to the energy of the outgoing proton. In the above equation T_0 is the kinetic energy of the incident proton, V_0 is the average nuclear well depth, 20 MeV in this case, and B is a nuclear binding term, 9 MeV in this case. In the present analysis a slightly modified Gaussian formula

$$N(E) = N_0 e^{-(E-E_x)^2/\lambda}(1-e^{-\alpha E}) \quad (6)$$

was used which includes a low excitation energy cutoff factor. The cutoff factor simulates the effects of Pauli blocking and Fermi averaging. The parameter $\alpha \approx \frac{1}{4}$ MeV in the cutoff factor was chosen to give a reasonable fall off at low excitation energy. The width of the Gaussian was chosen to give a reasonable fit for the continuum in the giant resonance region, and, as was observed[7] at 200 MeV, it increases with scattering angle. The background at excitations above the centroid was described by a fourth-order polynomial drawn smoothly through the data. The quantity N_0 is the value of the polynomial fit at the quasielastic centroid. We emphasize that the procedure of using a Gaussian connected to a polynomial does not depend solely upon the quasielastic scattering hypothesis, but is simply an empirical approach to fitting the observed spectra.

IV. RESULTS AND ANALYSIS

Representative fits of the measured 400-MeV spectra at 6° and 10° using the Gaussian plus polynomial background prescription of Eq. (6) are shown in Fig. 2. The fits show the multipolarity decomposition of the giant resonance region. The 6° spectrum is dominated by the well-studied ISGQR at 10.6 MeV and the unresolved ISGMR and IVGDR at 14.0 MeV. The $2\hbar\omega$ hexadecapole resonance (ISGHR) previously observed at 200 MeV (Ref. 7) and 334 MeV (Ref. 9) is again seen at 12.0 MeV. As was the case at 200 MeV the width of the Gaussian is slightly broader for larger angles. In fitting the excitation region below 15 MeV it was assumed that only the four modes mentioned contribute significantly. Their resonance energies E_R and widths Γ_R were then chosen to be consistent with previous studies[7,9] and the strength of the various modes were allowed to vary to give the best overall fit to the measured spectra. The resonance parameters are summarized in Table I. From Fig. 2 it is seen that the giant resonance region up to about 15 MeV is adequately described with the above-mentioned resonant components.

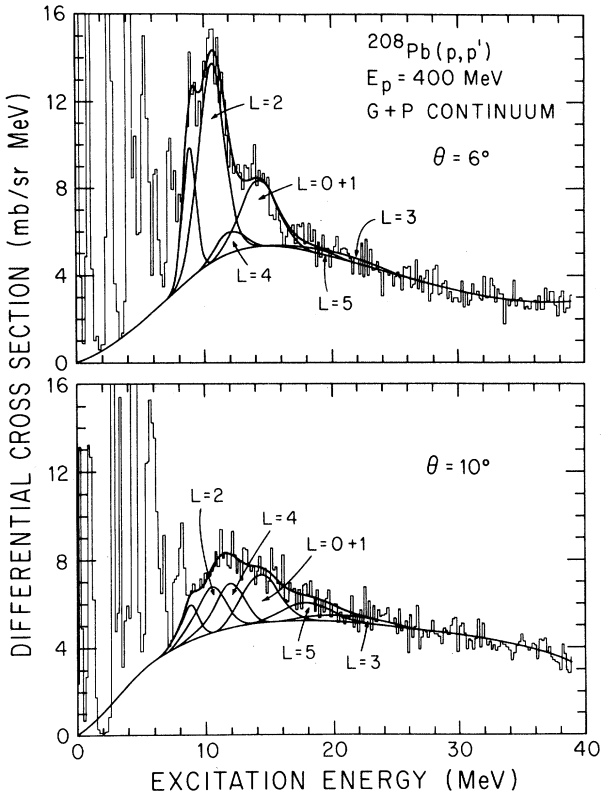

FIG. 2. Spectra of 400-MeV protons scattered from a ^{208}Pb target at laboratory angles 6° and 10°. The background curve corresponds to a Gaussian plus polynomial approach to the continuum. A multipole decomposition of the giant resonance region has been made and the position and multipolarity of the various components labeled. The composite curve of all components was constrained to fit the data.

The angular distribution for the ISGQR is shown in Fig. 3. The theoretical angular distribution curve shown

TABLE I. Values of the 400-MeV resonance parameters.

L		E_R (MeV)	Γ_R (MeV)	EWSR (%)
2	ISGQR	10.6	2.2	60±12
4	ISGHR	12.0	2.4	12±3
3	ISGOR	20.9	6.0	17±4
5		18.0	5.0	10±3

here, and for all subsequent figures were obtained using ECIS79.[28] A first-order vibrational model was used in the collective DWBA calculations, the same as in our previous work.[7,9,11] The transition potential comes from the distortion of the five separate terms of the optical potential (real, imaginary, real spin-orbit, imaginary spin-orbit, and Coulomb). The magnitude of the cross section is determined by the square of the deformation length, βR, used in the calculation. Each of the five terms of the optical potential has a deformation length associated with it: $(\beta_L^R R_R, \beta_L^I R_I, \beta_L^{\mathrm{RSO}} R_{\mathrm{RSO}}, \beta_L^{\mathrm{ISO}} R_{\mathrm{ISO}}, \beta_L^C R_C)$, where $R_x = r_x A^{1/3}$ with r_x being the appropriate radius for each of the five terms. In our calculations all of the deformation lengths were set to the same value. The sum rule limit (100% of the EWSR fraction) for giant resonances of angular momentum transfer $L \geq 2$ corresponds[29] to

$$(\beta_L R)^2 = \left[\frac{2\hbar^2\pi}{3m}\right] \frac{L(2L+1)}{AE_x} . \tag{7}$$

The ratio of the experimental cross section to the 100% DWBA cross section, obtained using the deformation length of Eq. (7) gives the sum-rule fraction.

An EWSR fraction of (60±12%) is found for the

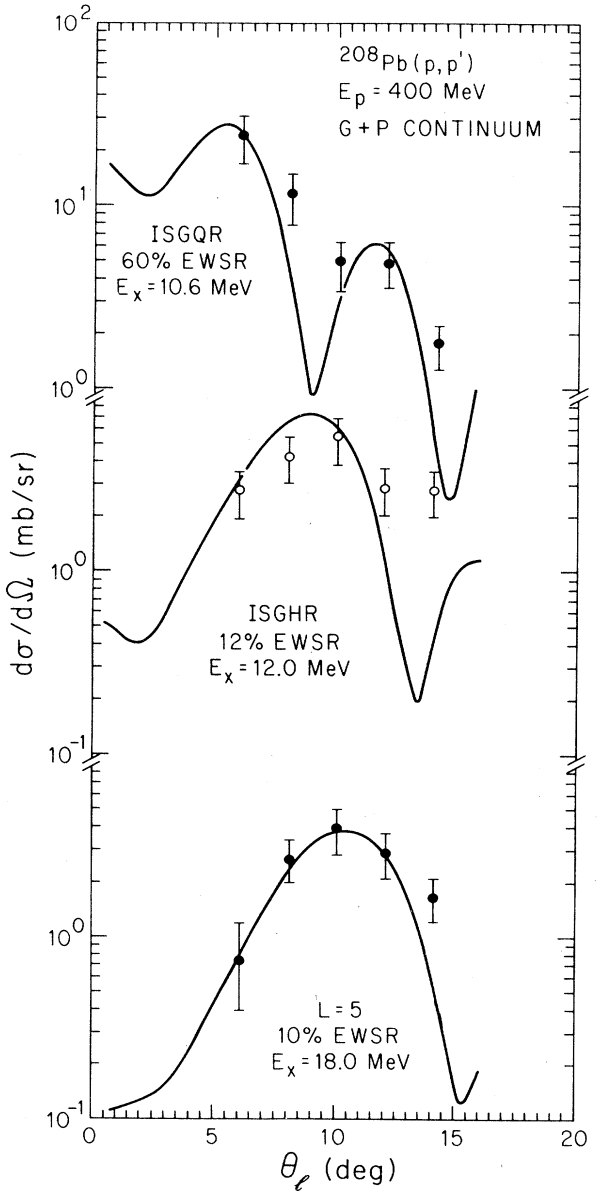

FIG. 3. Angular distributions of the ISGQR at 10.6-MeV, ISGHR at 12.0-MeV, and $L=5$ resonance at 18.0-MeV excitation for 400-MeV protons. The Gaussian plus polynomial approach was used for the background. The solid curves are DWBA predictions for the percent of EWSR strengths as labeled.

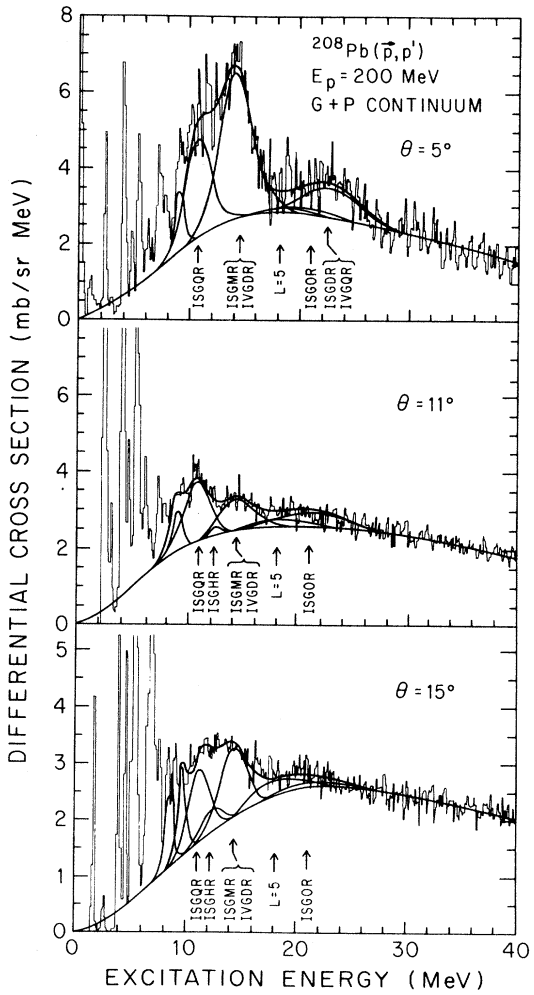

FIG. 4. Spectra of 200-MeV protons scattered from a ^{208}Pb target at laboratory angles of 5°, 11°, and 15°. The background curve corresponds to a Gaussian plus polynomial approach to the continuum. A multiple decomposition of the giant resonance region has been made and the position of the various multipole components labeled. The composite curve of all components was constrained to fit the data.

ISGQR using the Gaussian plus polynomial background subtraction method. This agrees well with our previous results at 200 MeV (65±15%) and 334 MeV (70±14%). The result at 200 MeV was obtained using the Gaussian plus polynomial model to describe the continuum, while the high resolution data obtained at 334 MeV were analyzed by drawing in a reasonable estimate of the background.

Figure 3 also shows the angular distribution for the ISGHR resonance. An EWSR fraction of (12±3%) is found, again in excellent agreement with the 200-MeV result of 8±3% and the 334-MeV result of 10±3%.

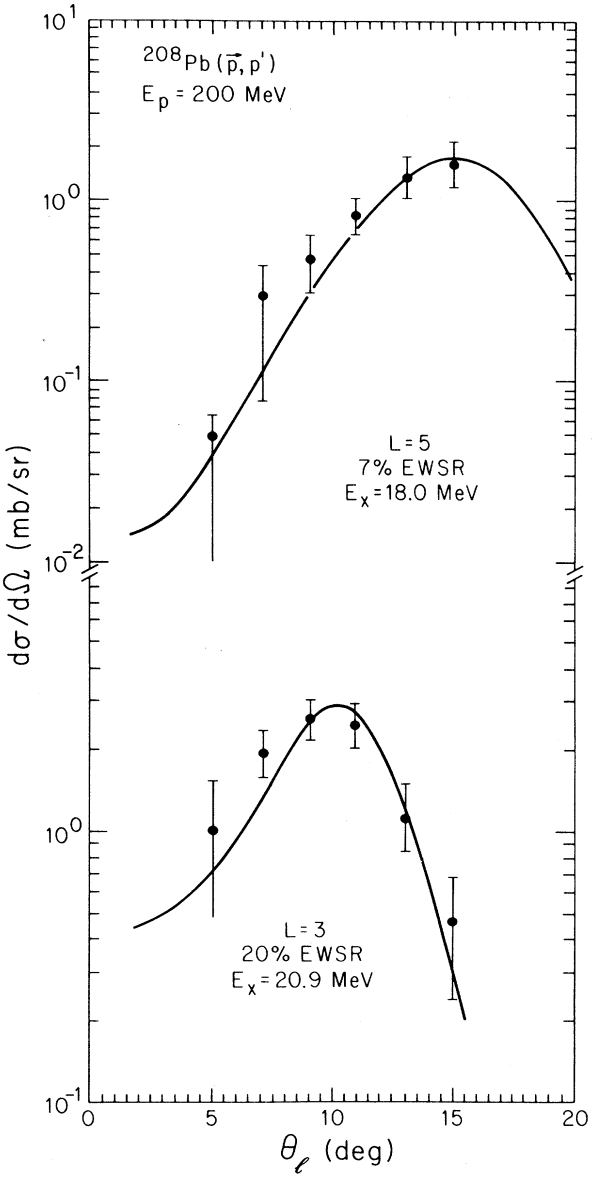

FIG. 5. Angular distributions of the $L=5$ at 18.0 MeV and $L=3$ ISGOR at 20.9-MeV excitation for 200-MeV protons. The Gaussian plus polynomial approach was used for the background. The solid curves are DWBA predictions for the percent of EWSR strengths as labeled.

As outlined in the introduction the exact multipolarity composition of the resonance structure in the excitation region from 15 to 25 MeV is more controversial and requires careful study. Contributions to this region may arise from the previously suggested ISGOR, $3\hbar\omega$ $L=5$ resonance, ISGDR, IVGQR as well as other high multipole resonance strength. Our earlier analysis[7] of the 200-MeV data places the ISGOR at 20.9 MeV with a width of 5.9 MeV. The ISGDR and IVGQR would only be expected to be observed at very forward angles because they are only weakly excited by the nuclear potential, but are much more strongly excited by Coulomb excitation. In the present experiment the 15–25-MeV region of the spectra in Fig. 2 were best fit by including a peak at 18 MeV, with a width of 5 MeV, in addition to the ISGOR. The fits to the spectra are improved at all angles with the inclusion of this peak. In the fitting procedure the parameters $E_R=20.9$ MeV and $\Gamma_R=6.0$ MeV for the ISGOR were taken from previous studies.[7] The resonance location of $E_R=18.0$ MeV is assumed and all other quantities are allowed to vary to obtain the best overall fit to the measured spectra. The angular distribution of the 18-MeV resonance is shown in Fig. 3. The data are best fit by an $L=5$ angular distribution which accounts for 10±3 % of the EWSR.

The 200-MeV data have been reanalyzed with the inclusion of the 18-MeV resonance and the ISGDR or IVGQR at 22 MeV. Representative spectra and the giant resonance multipolarity decompositions are shown in Fig. 4. The Gaussian plus polynomial approach was utilized to represent the continuum and the same fitting procedure followed as described above. The ISGDR (or IVGQR) is observed prominently only in the most forward 5 degree spectrum. The sum-rule fraction based on this one angle is 80±20 %. The $L=5$ and $L=3$ ISGOR angular distributions are shown in Fig. 5. The EWSR fractions shown for these resonances are consistent with

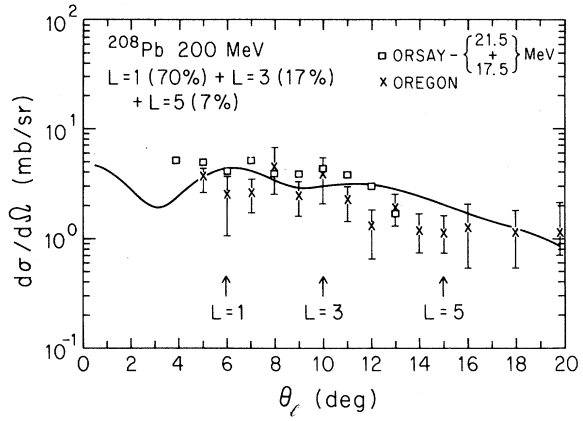

FIG. 6. Composite angular distribution of the 15–25-MeV excitation energy region for two experiments at 200-MeV. The open-square data points refer to Ref. 4 and the crosses refer to Ref. 7. The solid curve is the DWBA prediction for a weighted mixture of L values. The angles at which the various L-value components have their maxima are indicated by arrows in the figure.

TABLE II. Values by which the free-surface response calculations are renormalized.

Angle	Normalization
6°	.80
8°	1.13
10°	1.03
12°	.95
14°	1.3

those observed at 400 MeV. By including the 18-MeV resonance in our analysis an EWSR strength of 20±7 % is found for the ISGOR, which is to be compared with 36±12 % reported in our earlier analysis.

With the inclusion of three multipole components $L=1$, 3, and 5 in the 15–25-MeV region the ambiguity between the earlier analysis (based on $L=3$ only) of the 200-MeV data[7] and the analysis (based on $L=1$ plus $L=3$) of an experiment at 201 MeV is removed. The agreement is illustrated in the composite plot of Fig. 6, which shows the angular distribution of the integrated 15–25-MeV strength (as discussed in Ref. 7, Table III). The results of the 201-MeV experiment[4] (renormalized), including both 17.5 and 21.5 structures, are shown together with the 200-MeV data.[7] The calculated DWBA cross section shown corresponds to the combination of L

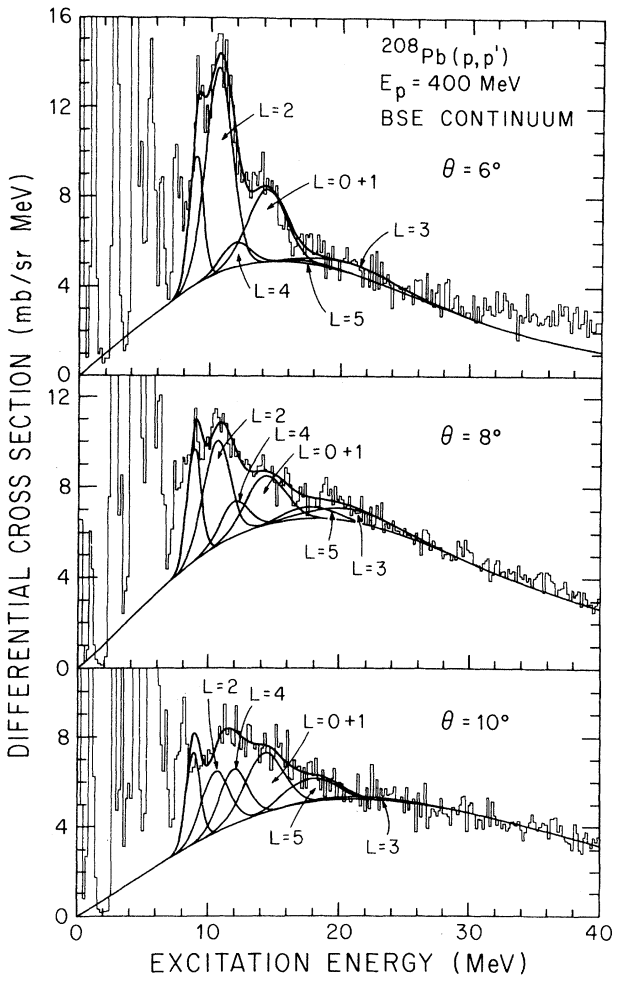

FIG. 7. Spectra of 400-MeV protons scattered from a ^{208}Pb target at laboratory angles 6°, 8°, and 10°. The background curve corresponds to the semi-infinite slab model [Bertsch, Scholten, and Esbensen (BSE)] approach to the continuum. The same multipole decomposition of the giant resonance region was made as in Fig. 1.

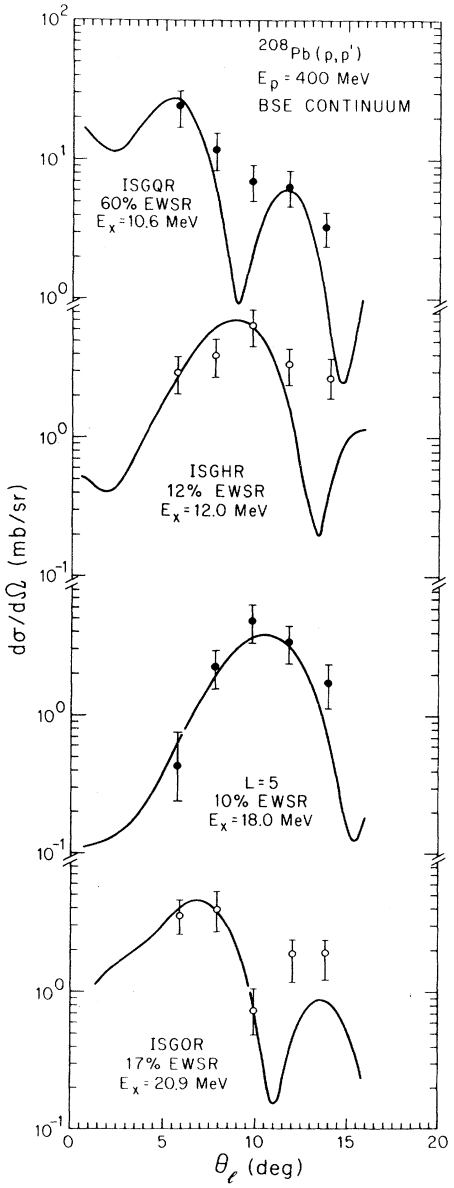

FIG. 8. Angular distributions of the ISGQR at 10.6-MeV, ISGHR at 12.0-MeV, $L=5$ at 18.0-MeV and ISGOR at 20.9-MeV excitation for 400-MeV protons. The semi-infinite slab model approach (BSE) was used for the background. The solid curves are DWBA predictions for the percent of EWSR strengths as labeled.

values and EWSR weighting determined from the new 200- and 400-MeV analyses presented above. It may be seen that the data in the 15–25-MeV region from the two experiments are now in agreement within uncertainty as well as with the combined DWBA prediction.

Our 400-MeV data have also been analyzed using the predictions of the surface response model[20] for the continuum. The actual calculations were done with a program using the nuclear free response approximation in a slab geometry.[22] The continuum predictions and the extracted resonance peaks are presented in Fig. 7. The continuum predictions were adjusted to the actual data to give a reasonable representation of the high excitation region. The required normalization factors are presented in Table II. With these empirical renormalizations the shape and magnitude of the continuum are well-described by the model for 400-MeV incident protons.

The same fitting procedure and multipole decomposition of the noncontinuum component are utilized in Fig. 7 for the giant resonance region as was used in Fig. 2. The resonance parameter summary of Table I is again appropriate. Figure 8 shows the resulting angular distributions. For the ISGQR, an EWSR fraction of 60±12 % is found, exactly the same as obtained from the Gaussian plus polynomial continuum analysis. The ISGHR strength of 12±3 % of the EWSR is also the same as was found from the phenomenological analysis. As with the phenomenological approach the 12° and 14° points of the ISGHR angular distribution are higher than the calculation for an $L=4$ transfer. This may suggest the presence of $2\hbar\omega$ $L=6$ strength near 12 MeV excitation as has been mentioned by Morsch *et al.*[13] For 400-MeV protons an $L=6$ resonance has its first maximum near 12°. However, larger angle data with good statistics are needed in order to confirm this suggestion.

Figure 8 also shows the angular distribution for the resonance at 18 MeV which is most prominent in the 10° spectra of Fig. 7. This resonance is again described well by an $L=5$ angular momentum transfer. The corresponding EWSR agrees within uncertainty with the value found from the phenomenological approach. Figure 8 also shows the angular distribution for the $3\hbar\omega$ ISGOR resonance at 20.9 MeV which accounts for 17±4 % of the EWSR.

Relativistic impulse approximation predictions[23] for the continuum are compared to those of the free-surface response and to representative 400-MeV ^{208}Pb data in Fig. 9. The two continuum calculations agree with each other and with the data only at large scattering angles. At smaller angles the relativistic predictions are not in such good agreement with the data, which is probably due to the approximation of using a Fermi-gas response function in the relativistic calculations. Improvements in the Dirac calculation may be expected by explicitly taking the nuclear surface into account.[30]

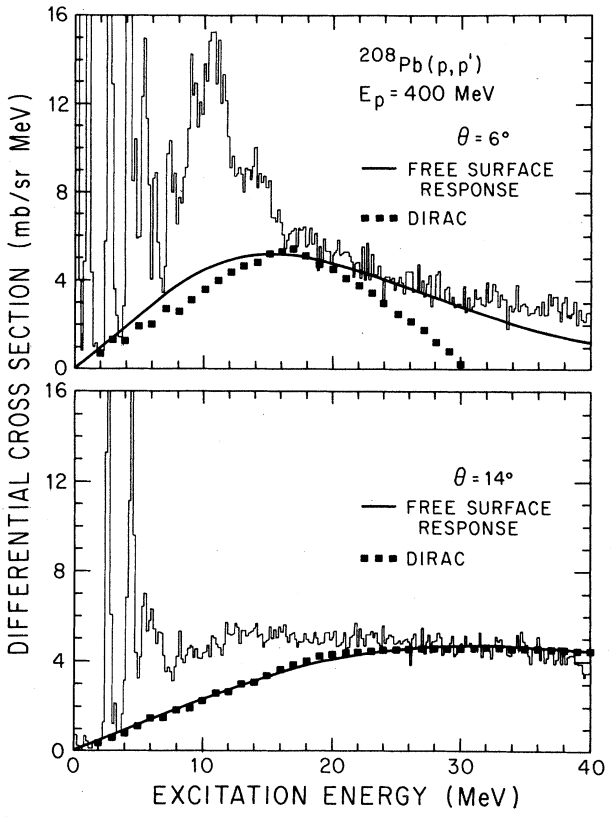

FIG. 9. Spectra of 400-MeV protons scattered from ^{208}Pb at laboratory angles 6° and 14° compared to calculated continuum cross sections. The solid curve corresponds to the semi-infinite slab model (BSE) of Bertsch, Scholten, and Esbensen and the solid-square points are the predictions of the Dirac based model of Horowitz and Iqbal.

V. DISCUSSION AND CONCLUSIONS

Two different methods have been used to model the underlying continuum in the giant resonance region. One empirical method uses a Gaussian shape to describe the excitation energy region at and below the empirically determined maximum in the data.[17] This method has previously been employed successfully in a ^{208}Pb(p,p') study[7] with 200-MeV protons. Analysis of our 400-MeV data using the phenomenological continuum description resulted in EWSR depletions for the established giant resonances which are in substantial agreement with our earlier results measured at 200 and 334 MeV.

The second method used to describe the continuum is based on the free-surface response of semi-infinite nuclear matter as developed by Bertsch, Esbensen, Scholten,[20–22] and Smith.[26] Good fits were obtained for the new 400-MeV continuum spectra. The giant resonance parameters obtained using the semi-infinite slab model are essentially the same as those obtained with the empirical Gaussian plus polynomial background approach. Hence, both methods work equally well in modeling the continuum at least so far as studies of the giant resonance region are concerned.

The results obtained here for the giant resonance parameters using both background procedures agree very well with published values from other experiments. Specifically, both methods find an EWSR fraction of

60±12 % for the ISGQR. This value is to be compared with 65±15 % obtained at 200 MeV,[7] 70±14 % at 334 MeV,[9] and 47±7 % at 800 MeV.[8]

Since both approaches to the background continuum lead to the same EWSR fractions for the prominent giant resonances, which are in good agreement with previous work at other energies, the results justify confidence in these methods of describing the underlying continuum in the giant resonance region. The theoretical approach based on the surface response might be preferred since it is a model calculation based on fundamental NN scattering and is less subject to individual subjective preferences. The good agreement for resulting EWSR fractions also reinforces some earlier work demonstrating the reliability of the DWBA collective model formalism for describing inelastic proton scattering to low-lying collective states at intermediate energies.[11,18,31]

As noted above the calculated continuum spectra of Fig. 7 have been renormalized to obtain the best fit to the data at high excitations above the giant resonances. It was found that it is not possible to fit the spectra at all angles with the same renormalization factor. The need for such a renormalization has been suggested by the work of Esbensen and Bertsch[21] in fitting inclusive (p,p') spectra in the 300–500-MeV range. Several factors which have not been completely incorporated into the free-surface response model may contribute to this need for renormalization. Medium modifications of Pauli blocking and residual particle-hole interactions can modify the total cross section $\sigma_{\rm NN}$ in Eq. (2) and the elastic differential cross section $d\sigma_{\rm NN}/d\Omega$ in Eq. (1). For all of the angles studied here, only Pauli blocking effects on $\sigma_{\rm NN}$ have been included, otherwise the free values have been used. The effect of Pauli blocking on $\sigma_{\rm NN}$ has been investigated by Esbensen and Bertsch[20,21] in a local Fermi gas model. It was found to decrease the value of $\sigma_{\rm NN}$ from the free value, thereby enhancing the calculated continuum cross section of Eq. (1) by about 20% when residual interactions are neglected. The effect of including residual interactions is to increase $\sigma_{\rm NN}$ and decrease the prediction of Eq. (1) by a smaller amount. The estimated effect of including residual interactions would thus be opposite to Pauli blocking effects at 400 MeV and hence partially offsetting. These conclusions are based on the use of a local Fermi gas approximation for the surface response function in calculating $\sigma_{\rm NN}$. These medium corrections should also be made to the interaction $d\sigma_{\rm NN}/d\Omega$ between the projectile and the nucleons in the target nucleus. The yield from Eq. (1) is expected[20,21] to decrease only slightly at large momentum transfers as a result.

An additional likely explanation for the need to renormalize Eq. (1) lies in the approximations made in calculating $N_{\rm eff}$, since it scales $d^2\sigma/d\Omega\,dE$. The straight line trajectory assumption may not be valid for larger angles. Also, the quantity $n(b)\sigma_{\rm NN}$ in the exponential of Eq. (2), which is related to the mean-free path, could also depend on the momentum transfer. Above all, the parametrization of the number of target nucleons per unit volume in the slab as independent of momentum transfer may also not be completely reliable. These considerations imply that $N_{\rm eff}$ may change with angle, and that it should in fact be considered a variable parameter.

The present application of the model uses only single-step scattering. For the higher excitation energies, and especially for the larger angles, multistep scattering becomes important. Esbensen and Bertsch[25] have estimated that the contributions of double scattering, for the momentum transfers and excitation energies we have studied, give a 10–20 % enhancement to the cross section. All the renormalization factors listed in Table II fall within the range of the above mentioned possible corrections.

Finally, we find the interesting possibility of a $3\hbar\omega$, $L=5$ resonance located at 18 MeV with a width of 5 MeV which exhausts 10±3 % of the EWSR. The calculation of Serr, Bortignon, and Broglia,[32] based on theoretical strength functions, indicate that a $3\hbar\omega$ $L=5$ resonance exhausting 12% of the EQSR should be expected near 20-MeV excitation. Experimental evidence for an $L=5$ resonance between 16- and 26-MeV excitation has also been observed by Bonin *et al.*[14] in (α,α') scattering. The EWSR fraction found in the alpha-particle experiments was 26±20 % for 340-MeV and 16±9 % for 480-MeV alpha particles.

ACKNOWLEDGMENTS

We have benefited from discussions on quasifree scattering with C. H. Horowitz, and the semi-infinite slab code was provided by H. Esbensen. We would like to thank TRIUMF staff members A. Miller, R. Abegg, and D. Hutcheon for their considerable assistance with the MRS facility. The University of Oregon and Oregon State University participants were supported in part by grants from the National Science Foundation. The Oak Ridge National Laboratory participants were supported by Martin Marietta Energy System, Inc. under U.S. Department of Energy Contract DE-AC05-84OR21400.

*Present address: Indiana University Cyclotron Facility, 2401 Milo Sampson Lane, Bloomington, IN 47408.

†Also affiliated with Simon Fraser University, Burnaby, B.C. Canada V5A 1S6.

[1]N. Marty, M. Morlet, A. Willis, V. Comparat, and R. Frascaria, Nucl. Phys. **A238**, 93 (1975).

[2]T. A. Carey, W. D. Cornelius, N. J. DiGiacomo, J. M. Moss, G. S. Adams, J. B. McClelland, G. Pauletta, C. Witten, M. Gazzaly, N. Hintz, and C. Glashauser, Phys. Lett. **45**, 239 (1980).

[3]F. E. Bertrand, E. E. Gross, D. J. Horen, J. R. Wu, J. Tinsley, D. K. McDaniels, L. W. Swenson, and R. Liljestrand, Phys. Lett. **103B**, 326 (1980).

[4]C. Djalali, N. Marty, M. Morlet, and A. Willis, Nucl. Phys. **A380**, 42 (1982).

[5]J. Tinsley, D. K. McDaniels, J. Lisantti, L. W. Swenson, D. M. Drake, R. Liljestrand, F. E. Bertrand, E. E. Gross, D. J. Horen, and T. Sjoreen, Phys. Rev. C **28**, 1417 (1983).

[6]S. Kailas, P. P. Singh, D. L. Friesel, C. C. Foster, P. Schwandt, and J. Wiggins, Phys. Rev. C **29**, 2075 (1984).

[7]D. K. McDaniels, J. R. Tinsley, J. Lisantti, D. M. Drake, I. Bergqvist, L. W. Swenson, F. E. Bertrand, E. E. Gross, D. J. Horen, T. P. Sjoreen, R. Liljestrand, and H. Wilson, Phys. Rev. C **33**, 1943 (1986).

[8]G. S. Adams, T. A. Carey, J. B. McClelland, J. M. Moss, S. J. Seestrom-Morris, and D. Cook, Phys. Rev. C **33**, 2054 (1986).

[9]F. E. Bertrand, E. E. Gross, D. J. Horen, R. O. Sayer, T. P. Sjoreen, D. K. McDaniels, J. Lisantti, J. Tinsley, L. W. Swenson, J. B. McClelland, T. A. Carey, K. Jones, and S. J. Seestrom-Morris, Phys. Rev. C **34**, 45 (1986).

[10]F. E. Bertrand, TRIUMF Report No. TRI-83-3, 1983.

[11]D. K. McDaniels, J. Lisantti, J. Tinsley, I. Bergqvist, L. W. Swenson, F. E. Bertrand, E. E. Gross, and D. J. Horen, Phys. Lett. **162B**, 277 (1985).

[12]H. P. Morsch, M. Rogge, P. Turek, and C. Mayer-Böricke, Phys. Rev. Lett. **45**, 337 (1980); H. P. Morsch, C. Sükösd, M. Rogge, P. Turek, H. Machner, and C. Mayer-Böricke, Phys. Rev. C **22**, 489 (1980).

[13]H. P. Morsch, P. Decowski, M. Rogge, J. Meissburger, and J. G. M. Römer, Phys. Rev. C **28**, 1947 (1983).

[14]B. Bonin, N. Alamanos, B. Berthier, G. Bruge, H. Faraggi, D. Legrand, J. C. Lugol, W. Mittig, L. Aapineau, A. I. Yavin, D. K. Scott, M. Levine, J. Arvieux, L. Farvacque, and M. Buenerd, Nucl. Phys. **A430**, 349 (1984).

[15]T. Yamagata, S. Kishimoto, K. Yuasa, K. Iwamoto, B. Saeki, M. Tanaka, T. Fukuda, I. Miura, H. Inoue, and H. Ogoto, Phys. Rev. C **23**, 937 (1981).

[16]J. Wambach, V. Klemt, and J. Speth, Phys. Lett. **77B**, 245 (1978).

[17]J. Lisantti, J. R. Tinsley, D. M. Drake, I. Bergqvist, L. W. Swenson, D. K. McDaniels, F. E. Bertrand, E. E. Gross, D. J. Horen, and T. P. Sjoreen, Phys. Lett. **147B**, 23 (1984).

[18]D. K. McDaniels, J. Lisantti, I. Bergqvist, L. W. Swenson, X. Y. Chen, D. J. Horen, F. E. Bertrand, E. E. Gross, C. Glover, R. Sayer, B. L. Burks, O. Häusser, and K. Hicks, Nucl. Phys. **A467**, 557 (1987).

[19]J. M. Moss, T. A. Carey, J. B. McClelland, N. J. DiGiacomo, S. J. Seestrom-Morris, G. F. Bertsch, O. Scholten, G. S. Adams, M. Gazzaly, N. Hintz, and S. Nanda, Phys. Rev. Lett. **48**, 789 (1982).

[20]H. Esbensen and G. F. Bertsch, Ann. Phys. (N.Y.) **157**, 255 (1984).

[21]H. Esbensen and G. F. Bertsch, Phys. Rev. C **34**, 1419 (1986).

[22]G. F. Bertsch and O. Scholten, Phys. Rev. C **25**, 804 (1982).

[23]C. J. Horowitz and M. J. Iqbal, Phys. Rev. C **33**, 2059 (1986).

[24]D. A. Hutcheon, J. M. Cameron, R. P. Liljestrand, P. Kitching, C. A. Miller, W. J. McDonald, D. M. Sheppard, W. C. Olsen, G. C. Neilson, H. S. Sherif, D. K. McDaniels, J. R. Tinsley, L. W. Swenson, P. Schwandt, C. E. Stronach, and L. Ray, Phys. Rev. Lett. **47**, 315 (1981); D. A. Hutcheon, W. C. Olsen, H. S. Sherif, R. Dymarz, J. M. Cameron, J. Johnson, P. Kitching, P. R. Liljestrand, W. J. McDonald, C. A. Miller, G. C. Neison, D. M. Sheppard, D. K. McDaniels, J. R. Tinsley, L. W. Swenson, and C. E. Stronach, Nucl. Phys. **A483**, 429 (1988).

[25]H. Esbensen and G. F. Bertsch, Phys. Rev. C **32**, 553 (1985).

[26]R. D. Smith, Bull. Am. Phys. Soc. **31**, 1229 (1986).

[27]S. J. Wallace, *Adv. Nucl. Phys.* **12**, 135 (1981).

[28]J. Raynal (private communication).

[29]G. R. Satchler, Nucl. Phys. **A195**, 1 (1972).

[30]Relativistic random-phase approximation (RPA) response calculations are in progress; M. J. Iqbal (private communication).

[31]K. W. Jones, C. Glashauser, R. deSwiniarski, S. Nanda, T. A. Carey, W. Cornelius, J. M. Moss, J. B. McClelland, J. R. Comfort, J. L. Escudie, M. Gazzaly, N. Hintz, G. Igo, M. Haji-Saeid, and C. A. Witten, Jr., Phys. Rev. C **33**, 17 (1986).

[32]F. E. Serr, P. F. Bortignon, and R. A. Broglia, Nucl. Phys. **A393**, 109 (1983).